Synthesis and Conformational Transition of Surface-Tethered Polypeptide: Poly(L-glutamic acid)

Yuli Wang and Ying Chih Chang*

Department of Chemical Engineering and Materials Science, University of California, Irvine, California 92697-2575

Received January 24, 2003; Revised Manuscript Received June 4, 2003

ABSTRACT: Surface-grafted poly(L-glutamic acid) (PLGA) films on silicon oxide surfaces were prepared and examined for their responsiveness to the external stimuli of pH, surfactant (decylammonium chloride), and divalent metal ion (Ca^{2+}) in aqueous solutions. A surface-initiated vapor deposition−polymerization of *N*-carboxyanhydride of γ-benzyl L-glutamate was first performed to synthesize surface-grafted poly(γ-benzyl L-glutamate) (PBLG) thin films, followed by debenzylating with hydrogen bromide in anhydrous benzene. The successful conversion of surface-grafted PBLG to PLGA films was confirmed by Fourier transform infrared spectroscopy and ellipsometry. The conformational transitions and the corresponding changes in film thicknesses and refractive indices were in situ examined by circular dichroism (CD) and ellipsometry, respectively. The CD study shows that the conformation undergoes a transition between α-helix and random coil at pH 5.75−7. Upon the conformational transition, the film thicknesses and refractive indices change correspondingly. From pH 4 to 8, the helical chains with the average thickness of 170 nm and refractive index of 1.381 change to the random coils of 260 nm and 1.355. Compared to the solvated free PLGA chains, the grafted chains are in favor of helical conformation. The observations of the transitional behaviors induced by decylammonium chloride and Ca^{2+} lead to similar conclusions.

1. Introduction

The conformational transition of polypeptides among α-helix, β-sheet, and random coil has been a subject of extensive theoretical and experimental studies for more than four decades. With different side-chain compositions, the conformational transition can be induced by various stimuli, including pH,[1−3] surfactants,[4−6] ions,[7,8] heat,[9−11] solvents,[12] hydrogen-bonding reagents,[13,14] light,[15,16] etc.

When the polypeptide chains are terminally grafted on a solid surface, a novel structure is formed. While the molecular chains retain sufficient flexibility to undergo conformational transitions, the surface attachment improves the long-term film stability to ensure such transitions reversible and repeatable. The conformational transitions could induce the changes of surface molecular structures, which in turn bring on their functionality. Conceivably, a futuristic biocompatible, site-specific molecular device in command of external stimulants can be built accordingly. For instance, superior electrooptical and electromechanical efficiencies in surface-grafted polypeptide films exhibit only in the α-helical structure as a result of the additive dipole moments along the molecular axis;[17,18] hence, a switchable optic or electronic surface may be readily designed by regulating the thin film molecular conformation among different secondary structures.

Up to date, unlike other transitions such as the glass transition or the melting of polymer thin films which have been studied extensively,[19] the understanding in conformational transitions of surface-grafted ultrathin polypeptide films was lacking, partially due to the lack of effective approaches to synthesize surface-grafted polypeptides. In this study, we first focus on the development of chemical synthetic protocols to create surface-grafted polypeptide films of interest; second, we investigate conformational transitions of these systems.

As the first report of the series, a grafted film composed of poly(L-glutamic acid) (PLGA), a naturally occurring polypeptide with carboxylic acid side chains, is fabricated as our model system. Specifically, we synthesize this film by utilizing the surface-initiated vapor deposition−polymerization (SI-VDP) of *N*-carboxyanhydride (NCA) of γ-benzyl L-glutamate (BLG), developed and improved by Chang and coauthors.[20−23] This method has recently shown to be the most effective approach in synthesizing surface-grafted poly(γ-benzyl L-glutamate) (PBLG) films with controllable thicknesses from a few nanometers to submicrons.[21] Subsequently, the conversion of surface-grafted PBLG to PLGA films is accomplished by removing the γ-benzyl protection groups.

Motivated by the curiosity in biology, the helix−coil transition of solvated free PLGA chains has been studied extensively in the past; it was found that the cooperative transition between helix and coil can be regulated by the degree of ionization of carboxylic side chains—when they are protonated (neutralized), the molecular backbone is in favor of the regular helical structure stabilized by the hydrogen bonds between the repeating units i and $i + 3$; when deprotonated (ionized), the electrostatic repulsions among side chains destabilize the intramolecular hydrogen bonds, thus randomizing the regular conformation.[2,24] In other words, the helix−coil transition of PLGA can be attributed to the neutral−ionic transition of its carboxylic side chains. Hence, external stimulants that are able to neutralize or ionize the side chains would be able to induce the helix−coil transition of the polypeptide backbones, and such a transition is conceivably reversible. In this study, we use three known stimulants, (1) H^+/OH^- (pH),[25,26] (2) surfactant (decylammonium chloride (DAC)),[27−30] and (3) divalent metal ion (Ca^{2+}),[31,32] to induce the reversible helix−coil transition at surfaces, as schematically shown in Scheme 1.

10.1021/ma034092z CCC: $25.00
Published on Web 07/30/2003

Scheme 1. Schematic Illustration of the Reversible Helix−Coil Transition of a High-Density, Surface-Grafted PLGA Monolayer Induced by Typical External Stimulants

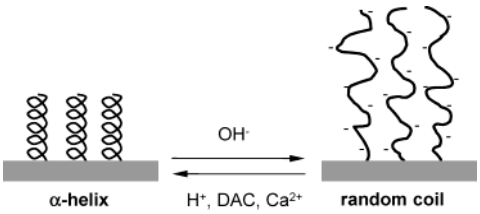

To utilize the conformational transition properties to construct stimuli-responsive "smart" surfaces, the correlation between conformations and the resulting surface properties has to be established. In our first attempt, the changes of surface dielectric properties are investigated. For this purpose, both in-situ measurements by circular dichroism (CD) for molecular conformations and ellipsometry for thickness and refractive index are applied.

2. Experimental Section

2.1. Synthesis of Surface-Grafted PLGA. Scheme 2 outlines the synthetic procedure for the surface-grafted PLGA on silicon and quartz substrates. Detailed information about chemicals, cleaning of substrates, and debenzylation is described in the Supporting Information.

(1) Silanization of the substrates. The immobilization of an (aminopropyl)triethoxysilane (APS) initiator layer onto the substrates was accomplished in the vapor phase under reduced pressure for 16 h following the procedure described previously.[21]

(2) Surface-initiated vapor deposition−polymerization (SI-VDP) of *N*-carboxyanhydride (NCA) of γ-benzyl L-glutamate (BLG). The SI-VDP process was carried out using the experimental setup described in the previous publication.[21] The following reaction condition was used: 8 mg of NCA of BLG was evaporated at 0.1 Pa for 10 min, with the NCA evaporating temperature at 95 °C and the substrate temperature at 60 °C. To remove the loosely bound materials, the films were sonicated in a mixture of dichloroacetic acid and chloroform (20/80 (v/v)) for 5 min, followed by rinsing with fresh chloroform and drying under a stream of nitrogen. The thickness of the resulting surface-grafted PBLG films on silicon substrates was 97.2 ± 0.5 nm measured by an ellipsometer.

(3) Conversion of surface-grafted PBLG to PLGA. The surface-grafted PBLG films were sonicated in HBr/benzene solution in a tightly sealed test tube for 1 h to remove the γ-benzyl protection groups. After the reaction, the substrates were rinsed with toluene, acetone, and distilled water and dried under a stream of nitrogen.

2.2. Characterization Methods. *Fourier Transform Infrared Spectroscopy (FTIR).* FTIR spectra of surface-grafted polypeptide films on silicon substrates were recorded using a Nicolet Magna-IR 860 spectrometer in transmission mode. Before and during the measurements, the sample chamber was purged with dry air (Whatman FT-IR purge gas generator). Spectra were recorded at 4 cm^{-1} resolution, and 32 scans were co-added.

Circular Dichroism (CD). CD (JASCO J-60 spectropolarimeter) was used to characterize the conformations of surface-grafted polypeptides on quartz substrates. The spectra were recorded at a bandwidth of 1 nm and a scanning rate of 20 nm/min. A rectangular demountable liquid cell (Starna Cells Inc.) with 1 mm path length was used. A cell holder was used to fix the quartz plate with the cell. The arrangement of the cell assembly and the beam path are shown in Scheme 3a. In this arrangement, the PLGA coated side is in contact with the filled solution, so that the film conformations can be measured in situ.

Ellipsometry. Ellipsometric measurements of the thin films on silicon substrates were performed with a Gaertner LSE stokes ellipsometer equipped with a He−Ne laser (λ = 632.8 nm) and a fixed incident angle of 70°. The film thicknesses and refractive indices were calculated from the measured ellipsometric angles (relative phase shift Δ and amplitude ratio ψ between the s- and p-polarized components of the probing laser) using the Gaertner Ellipsometer Measurement Program. Both dry and solvated films were measured. To measure the solvated PLGA film at the water−solid interface, a glass liquid cell (Gaertner Inc.) was used, whose schematic design is shown

Scheme 2. Schematic Diagram of the Pathway To Synthesize a Surface-Grafted PLGA Film with an Average Degree of Polymerization of *n*[a]

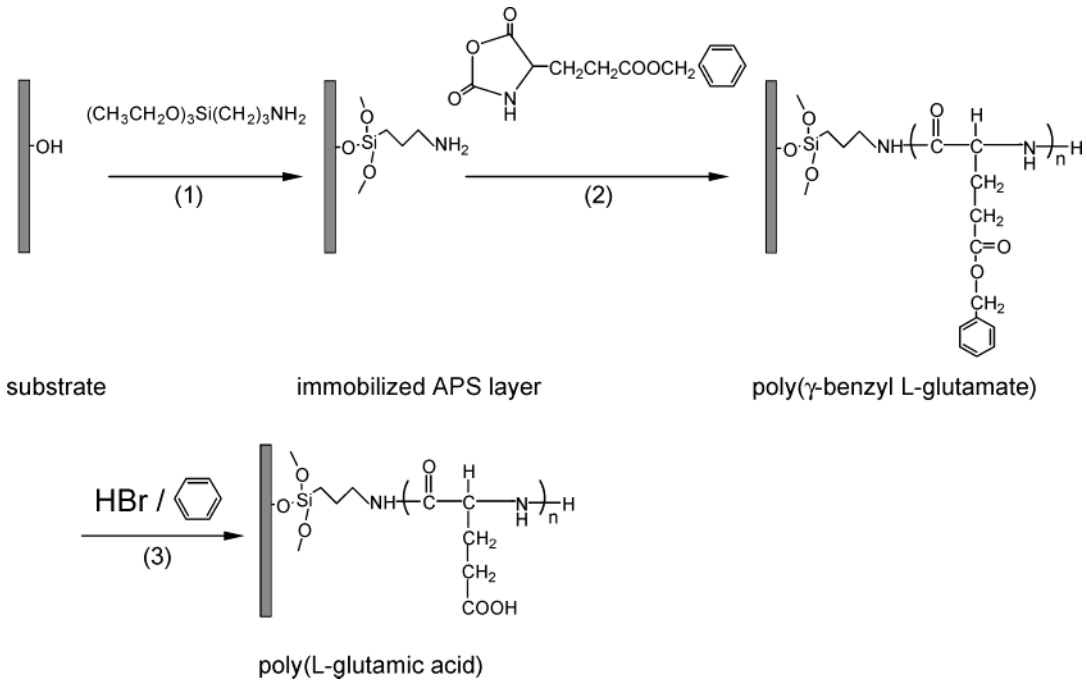

[a] (1) Vapor silanization of substrates with APS; (2) SI-VDP of NCA of BLG from the surface-bound APS; (3) debenzylation of the surface-grafted PBLG to form PLGA.

Scheme 3. Schematic Diagrams of the Experimental Configurations for (a) CD and (b) Ellipsometry[a]

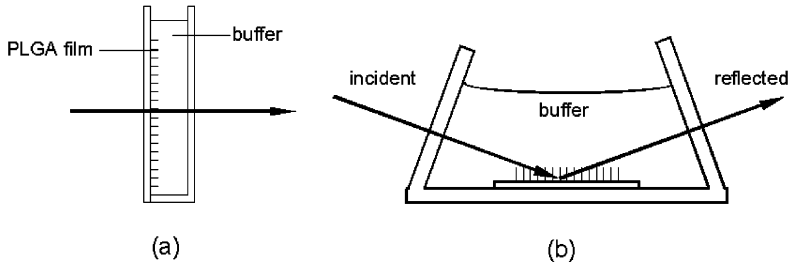

[a] The beam paths are indicated by the arrows.

in Scheme 3b. The laser beam passes through the entrance and exit windows at the normal angle so that the polarization of the probing laser beam is not altered by transmission through these windows. The substrate was placed on the bottom of the liquid cell, and the liquid cell was then fixed firmly on the measuring table. A 60 mL buffer (2 mM sodium phosphate or tris(hydroxymethyl)aminomethane (Tris)) solution was added into the cell, and the ellipsometric angles ψ and Δ were recorded as a function of time until equilibrium was reached. Further changes of the pH and composition of the bulk solution were achieved by adding external stimulants, such as H^+/OH^-, DAC, and Ca^{2+}. During this process, the ellipsometric angles were automatically recorded every 5 s. The measured ψ and Δ were analyzed by using an isotropic three-phase model (substrate/film/water) to calculate the film thickness and refractive index. The refractive indices of the aqueous phase (including all buffers) were simply taken as 1.333. (Because the film thickness in this study is rather large, this simplicity brings only negligible error.)

3. Results and Discussion

3.1. Synthesis of Surface-Grafted PLGA. The successful fabrication of grafted PLGA films was verified by both FTIR and ellipsometric measurements taken after the grafting of PBLG and the subsequent debenzylation, respectively. Figure 1a shows a typical FTIR spectrum of the grafted PBLG film in air with a thickness of 97 nm. Its α-helical conformation is evidenced by the locations of the amide I at 1653 cm^{-1} and amide II at 1549 cm^{-1}.

After debenzylation, the FTIR spectra of the resulting PLGA film in air were taken after treating with pH 4 and 8 buffers (2 mM sodium phosphate). We used pH

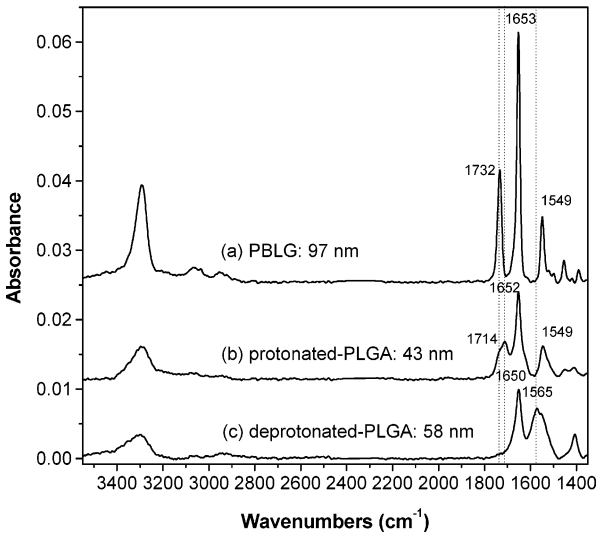

Figure 1. FTIR spectra of surface-grafted (a) PBLG (97 nm), (b) protonated PLGA (43 nm), and (c) deprotonated PLGA (58 nm) measured in ambient conditions.

treatments to guarantee the protonated or deprotonated state of the carboxylic side chains of PLGA because these two states show different IR characteristics. For the protonated PLGA film (Figure 1b), the peaks at 1652 and 1549 cm^{-1} attributed to the amide I and amide II absorbances, as well as the peak at 1714 cm^{-1} attributed to the carboxylic acid side chains, can be clearly distinguished. For the deprotonated PLGA film (Figure 1c), a broad peak centered at 1565 cm^{-1} is the convoluted peak by the carboxylate stretch at 1587 cm^{-1} and the amide II at 1542 cm^{-1}. Nevertheless, for both protonated and deprotonated PLGA films, their FTIR spectra show no absorbance at 1732 cm^{-1} (attributed to the γ-benzyl side groups of PBLG), confirming the complete conversion of PLGA from its precursor PBLG.

Conventionally, the debenzylation of PBLG was achieved by directly treating with anhydrous hydrogen bromide in glacial acetic acid.[33,34] However, this approach can severely damage surface-bound films at oxide surfaces due to the hydrolysis of Si−O bonds by the acetic acid. For instance, a 100 nm grafted PBLG film can be completely cleaved away after 16 h HBr/acetic acid treatment. To retain the film as much as possible while hydrolyzing the γ-benzyl ester side chains, a HBr/benzene solution was used in our study to ensure minimal film loss.

The ellipsometric thicknesses of the three films in air (PBLG, protonated PLGA, and deprotonated PLGA films) are indicated in Figure 1. It is interesting to note the PLGA film has different thickness in different protonation state: it has 43 nm in protonated state, while 58 nm in deprotonated state. The detailed explanation of the thickness discrepancy resulting from the conformation and packing density, as well as the CD spectra of these dry films, will be offered in section 3.3.5.

3.2. Overview: Helix−Coil Transition of Surface-Grafted PLGA. For an end-grafted PLGA chain, because only the terminal group is tethered at the surface, presumably, the rest of the chain would have sufficient degree of freedom for undergoing helix−coil transition. However, the thermodynamic and kinetic behaviors of the grafted chains might perform differently from those of the free chains. First of all, the fixation of the chain ends and surface effects might prevent a full transition. Second, the helical conformation in the grafting state might be more favorable than the random coiled conformation, due to the changes of boundary free energy and the van der Waals attractions among the grafted helices, as predicted by one theoretical model.[35] Kinetically, the diffusivity of external stimulants becomes a more dominant factor in films than that in free chain configuration in determining the transition rate; the large stimulant molecules would lead to a much slower transition. In addition, the confined space might pro-

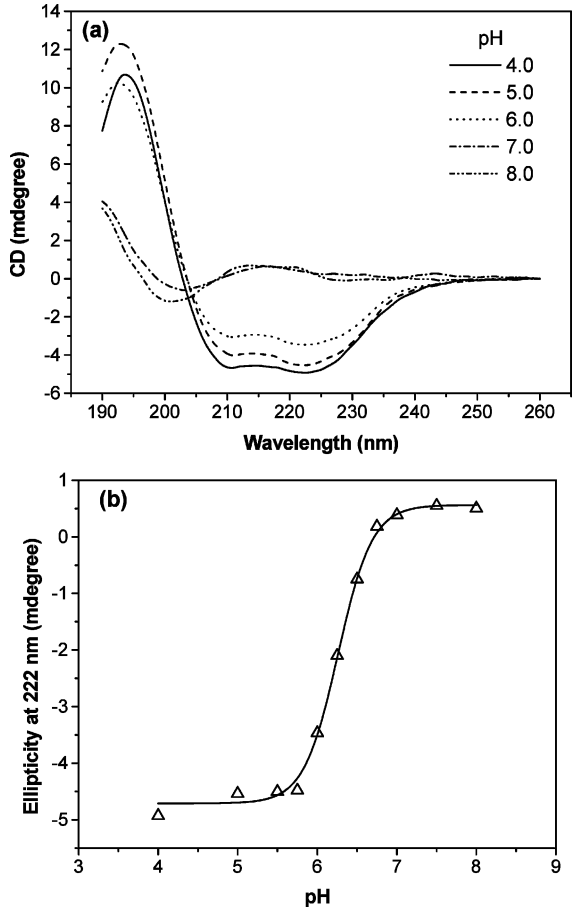

Figure 2. (a) CD spectra of a surface-grafted PLGA on a quartz plate in 2 mM sodium phosphate buffers from pH 4 to pH 8. (b) pH dependence of CD ellipticities at 222 nm.

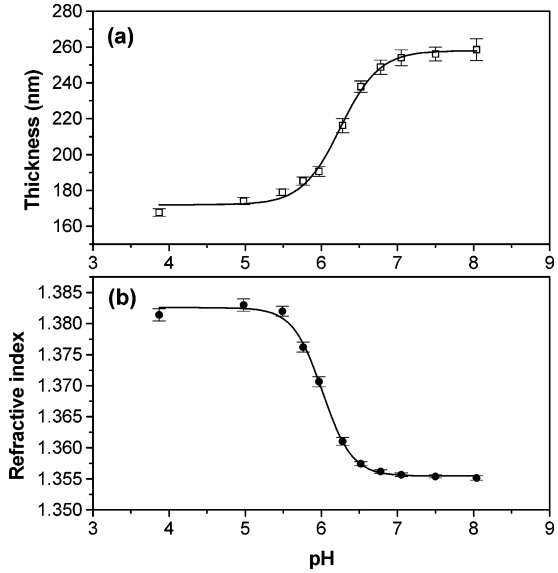

Figure 3. pH dependence of (a) ellipsometric thickness and (b) refractive index of a surface-grafted PLGA on a silcon substrate from pH 4 to pH 8.

mote chain movement preferentially along the surface normal, since the lateral directions are already crowded by the neighbor molecular chains.

In the following sections, we will experimentally examine the above-mentioned hypothesis and theoretical model by systematically changing environments. First, we will investigate the transition behavior induced by H^+/OH^-. Second, a larger molecule, a DAC surfactant, will be used to induce the transition to compare with the smaller stimulants of H^+/OH^-. Third, the biologically important ion, Ca^{2+}, will also be employed to further understand the conformational transition of the surface-grafted PLGA film.

3.3. Helix−Coil Transition Induced by pH. We used CD and ellipsometry to directly demonstrate the helix−coil transition occurred in the surface-grafted PLGA films. This result is further compared with that of the solvated free chains and the existing theoretical models.

3.3.1. CD. CD is used to characterize secondary structures of polypeptides. For an α-helical conformation, the CD spectrum shows double minima at 208 and 222 nm and a maximum at 196 nm. For a random coiled conformation, the CD spectrum shows two extrema with a maximum centered at 216 nm and a minimum at 200 nm.[36] Typically, the quantitative measurement of helical content is calculated from the mean molar ellipticity at 222 nm, $\theta_{mrd} = \theta_d/10lc_r$, where θ_d is the raw CD ellipticity, l is the path length, and c_r is the mean residue molar concentration.

Figure 2a is the collection of CD spectra of a surface-grafted PLGA in buffers from pH 4 to 8. The raw CD ellipticity is negatively large with $\theta_{222} = -4.9$ mdeg below pH 5, increasing rapidly between pH 5.75 and pH 6.5, and finally reaches a positive value of $\theta_{222} = 0.5$ mdeg above pH 7. To identify the helix−coil transition point, θ_{222} values were plotted against pH. (In the surface-grafted film, since the "surface concentration" is fixed and therefore c_r is constant, only the raw CD intensity is enough to calculate the helical content.) As shown in Figure 2b, the transition is clearly taken place between pH 5.75 and 7, with the inflection point at pH 6.25.

3.3.2. Ellipsometry. Ellipsometry was used to measure the thickness and refractive index of solvated films in response to different pH buffers. As plotted in Figure 3, the thickness of the surface-grafted PLGA increases from 170 nm at pH 4 to 260 nm at pH 8, while the refractive index decreases from 1.381 to 1.355. The transition of thickness occurs between pH 5.75 and pH 7, agreeing with the helix−coil transition observed from CD. (Note: the transition of refractive index occurs between pH 5.5 and 6.5, which is not the same as thickness. We think conformation is more closely correlated to thickness than refractive index, since the changes of refractive index also involve other factors such as the amount of water intake.)

Interestingly, ellipsometric data suggest that the grafted PLGA chains expand dramatically in the helix-to-coil transition. For solvated free chains, helical peptides are often modeled as the rodlike structure with the persistent length (l) proportional to the degree of polymerization (DP) ($l \sim DP^1$), and when being converted to random coils, the radius of gyration becomes proportional to the square root of molecular weight ($l \sim DP^{0.5}$).[37] On the contrary, in the grafting state, the tethered molecules are obliged to stretch away from the surface due to the surface crowded chains when being converted from helices to coils. Thus, instead of forming a coiled sphere, the one-dimensional movement leads to the formation of fully extended chains with the average thickness proportional to the DP. For the average length of repeating unit estimated to be 0.15

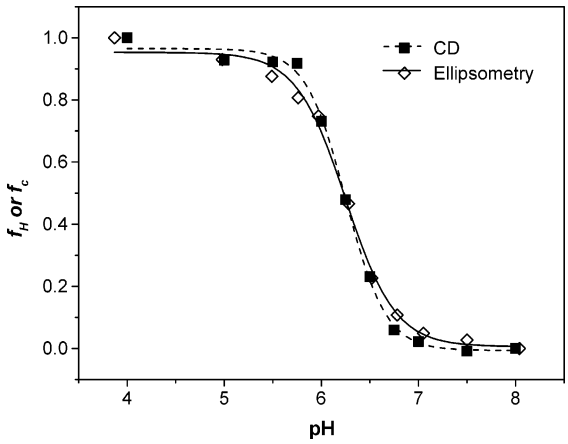

Figure 4. Equivalency of CD and ellipsometry in studying the pH-induced helix−coil transition for surface-grafted PLGA films on solid substrates.

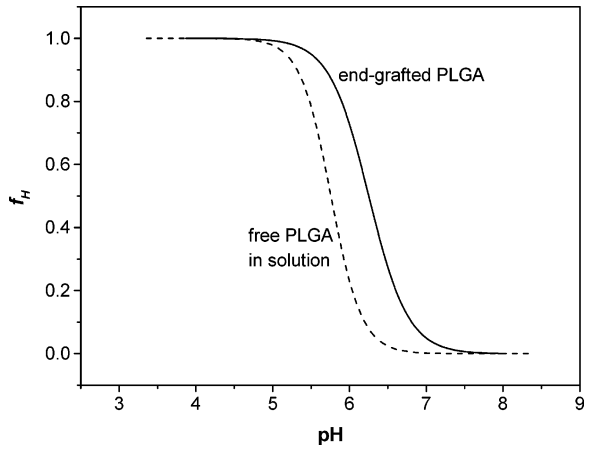

Figure 5. Comparison of the helix−coil transitional behavior induced by pH for PLGA in surface-grafting and free solution states. Only trend lines obtained from CD measurements are shown here. The dash transition curve is for free PLGA in an aquous solution (DP ≈ 105, 0.1 mg/mL) measured by CD.

nm for a helix and 0.35 nm for a random coil, with molecular diameters of 1.4 and 1.1 nm, respectively,[38] we can estimate the relationship of thickness (d) and DP as follows: In the helical conformation, $d_H \sim 0.15DP^1$ (nm); hence, we can estimate the DP of the grafted PLGA film of 170 nm to be about 1100. By the same approximation, the 170 nm helical rod would become 385 nm in a fully extended chain conformation, since $d_C \sim 0.35DP$. This value apparently is overestimated compared to the experimental value of 260 nm. To fit the experimental value, the random coiled thickness should be expressed by $d_C \sim (0.35DP)^{0.93}$. The index (0.93) suggests that the random-coiled PLGA chains indeed stretch away from the surface, but not fully.

The pH-induced helix−coil transition of the surface-grafted PLGA caused more than 50% relative dimensional change. This conceivably can have many interesting applications. Ito et al. have grafted PLGA on porous membranes to serve as a pH gating to regulate the water permeation rate by adjusting pH.[39,40] Their finding on porous membranes agrees with ours on flat surfaces.

3.3.3. Equivalency of CD and Ellipsometry. The relationship between the helix−coil transition and the changes of film thickness can be further quantified as follows:

For CD measurements, the fraction of helix (f_H) can be calculated as

$$f_H = \frac{\theta_C - \theta}{\theta_C - \theta_H} \tag{1}$$

where θ is the ellipticity at 222 nm, θ_H is the ellipticity at 222 nm for the α-helical PLGA at pH 4, and θ_C is the ellipticity at 222 nm for the random-coil PLGA at pH 8.

For ellipsometry measurements, we define the degree of compression, f_C, as

$$f_C = \frac{d_C - d}{d_C - d_H} \tag{2}$$

where d is the film thickness, d_H is the film thickness for the α-helical PLGA at pH 4, and d_C is the film thickness for the random-coil PLGA at pH 8.

Figure 4 shows f_H and f_C vs pH curves from both measurements for surface-grafted PLGA. These two curves coincide. This further confirms the strong correlation between the molecular conformation and surface properties. In addition, for this particular case, both CD and ellipsometer can be used to give fairly good measurements in characterizing the helix−coil transition.

3.3.4. Comparison of Transitional Behavior between Surface-Grafting State and Free State. For free PLGA with DP ∼ 105 in the aqueous solution, the pK_a value of carboxylic acid side groups is 4.375,[38] and the transition inflection point, pH_t, is about 5.74, as shown in Figure 5 (the dotted line).[41] Compared to the surface-grafted PLGA, where the transitional point pH_t shifts to alkaline side with the value of 6.25, the result suggests that the grafting state favors the helical state. The shift of transitional point might be explained as follows:

The helix−coil transition was theoretically described by the Zimm−Bragg model as[42]

$$f_H = \frac{1}{2}\left(1 + \frac{s-1}{[(s-1)^2 + 4\sigma_{ZB}s]^{1/2}}\right) \tag{3}$$

where σ_{ZB} is the initiating parameter reflecting the extra difficulty of initiating a helical section, which controls the cooperativeness of the transition; s is the propagation parameter which corresponds to the free energy of adding a helical unit to an existing helical region.

For free PLGA in an aqueous solution

$$-kT \ln s = \Delta f \tag{4}$$

where Δf is the free energy change on converting from the random coil to the helical form.

When the PLGA chains are immobilized on a solid surface, an extra free energy Δf_{extra} is associated.

$$-kT \ln s = \Delta f + \Delta f_{extra} \tag{5}$$

Δf_{extra} can be primarily divided into two parts for surface-grafted neutral polypeptides described by Buhot and Halperin:[35] Δf_w and Δf_{vdW}. Δf_w is the free energy penalty at the wall because of the presence of an impenetrable surface, and Δf_{vdW} is the change of van der Waals attraction between neighbor chains from random coils to helices, whose contribution is significant at high grafting density. For ionic polypeptide, an

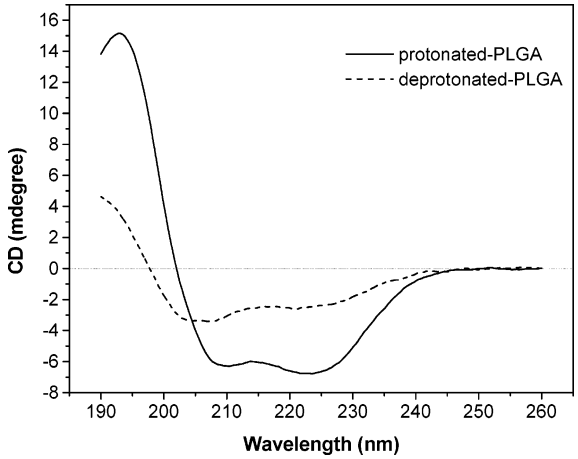

Figure 6. CD spectra of a dry surface-grafted PLGA on a quartz plate in both protonated and deprotonated state.

Table 1. Ellipsometric Measurements and Contact Angles of Surface-Grafted PBLG and PLGA

samples	thickness in dry film (nm)	refractive index in dry film	contact angle (deg)	thickness in pH 4 buffer (nm)
PBLG	97.2 ± 0.5	1.615 ± 0.004	70 ± 2	96.4 ± 0.4
protonated PLGA	43.0 ± 0.3	1.520 ± 0.002	55 ± 2	169.3 ± 0.8
deprotonated PLGA	57.9 ± 0.4	1.489 ± 0.001	4 ± 1	

additional part, Δf_{inter}, is significant in the grafting state. Δf_{inter} is the extra contribution from the intermolecular interaction, mainly electrostatic repulsion, in PLGA random coils in the grafting state. (This interaction is negligible in the dilute free PLGA solutions.) Therefore, for surface-grafted PLGA, Δf_{extra} is expressed as

$$\Delta f_{extra} = \Delta f_{w} + \Delta f_{vdW} + \Delta f_{inter} \quad (6)$$

The additional Δf_{extra} involved in surface-grafting state contributes to the shift of transitional point pH_t from the free state (pH 5.74) to the surface-grafting state (pH 6.25). In other words, when the PLGA chains are densely immobilized on surfaces, the stability of the helical state is reinforced. Our experimental data are consistent with the prediction of Buhot's model originally only applying for thermally induced helix−coil transition of surface-grafted neutral polypeptides.[35]

3.3.5. Surface Properties of PLGA Dry Films. The surface properties of the dry surface-grafted PLGA film were further investigated and are summarized in Table 1. The film was first treated with a pH 4 buffer (2 mM sodium phosphate) before dried in air. In this case, the water contact angle is 55°, the thickness is 43 nm, and the refractive index is 1.52. Interestingly, when the film was subsequently treated with a pH 8 buffer and then dried in air, the water contact angle decreases to only 4°, suggesting a completely hydrophilic surface. Furthermore, the thickness measured in air expands to 58 nm with the refractive index of 1.49. These results suggest that the dry films can preserve the protonated or deprotonated states based on the previous treatments.

The surface-properties of PLGA dry films can be related to the conformations presented in the films. Figure 6 shows the CD spectra of the dry PLGA films in the protonated and deprotonated state. As expected,

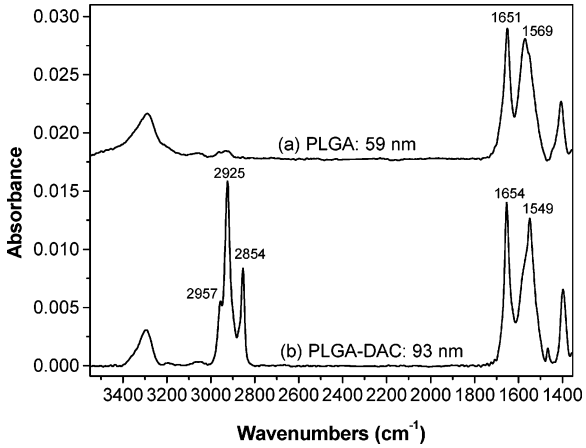

Figure 7. FTIR spectra of (a) a surface-grafted dry deprotonated PLGA (59 nm) and (b) PLGA−DAC complex (93 nm). To prepare the PLGA−DAC complex, the PLGA film was immersed in 10 mM DAC solution (buffered by 2 mM pH 8 Tris) for 20 min, taken out and rinsed by distilled water, and dried by a stream of nitrogen.

protonated PLGA adopts the α-helix structure, while deprotonated PLGA adopts a predominantly random-coil structure. This shows that the conformation in the solvated state can be retained in dry films. This also explains the discrepancy of ellipsometric measurements for the protonated and deprotonated PLGA.

In Table 1, the surface properties of PLGA films were further compared with those of the PBLG film before the debenzylation. Apart from the likely loss of films due to the hydrolysis of Si−O bonds, the removal of benzyl groups causes great reduction of the packing thicknesses and the refractive indices as well as the dramatic decrease in water contact angles in PLGA films. Further comparing the film properties in air and solution (pH 4 buffer), we found that a PLGA film with a thickness of 43 nm in air can be greatly expanded to 169 nm in a pH 4 buffer. On the other hand, there is no significant thickness change for a grafted PBLG film in both cases. This is due to the favorable interactions between the hydrophilic PLGA and water, so the molecular chains are fully stretched to maximize the contact with water molecules, while collapsing in air to minimize the surface energy. On the contrary, the hydrophobic PBLG−water interaction is not favorable; therefore, the film thicknesses in air and in buffer solution are similar.

3.4. Coil-to-Helix Transition Induced by Surfactant (DAC). The conformational transition of free PLGA on binding with cationic surfactants, decylammonium chloride (DAC) as an example, has been studied by CD and potentiometric titration.[27−30] It was found that the cooperative binding of DAC to PLGA causes the conformational transition from coil to α-helix when the degree of binding is above 0.55.

For surface-grafted PLGA, the diffusion of DAC molecules into the film has to be considered as the first step for the conformational transition to take place. Figure 7 shows the FTIR spectra of the surface-grafted PLGA and PLGA−DAC complex, with the dry film thickness labeled above each spectrum. The binding of DAC to PLGA is evident. The dry film thickness increases from 59 nm for deprotonated PLGA to 93 nm for the PLGA−DAC complex. The absorption peaks of the PLGA−DAC complex at 2957 (weak, CH_3, asymmetric, stretch), 2925 (strong, alkyl CH_2, asymmetric,

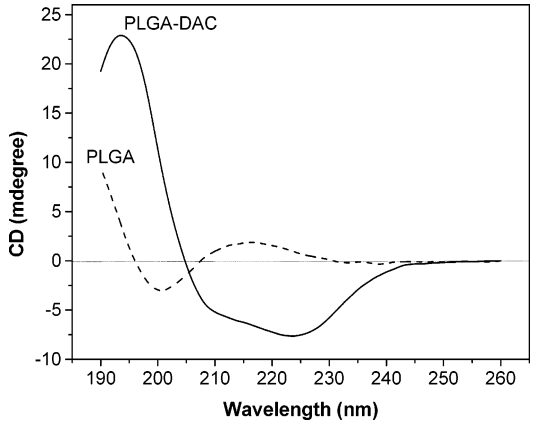

Figure 8. CD spectra of surface-grafted PLGA and PLGA−DAC complex in 2 mM pH 8 Tris buffer.

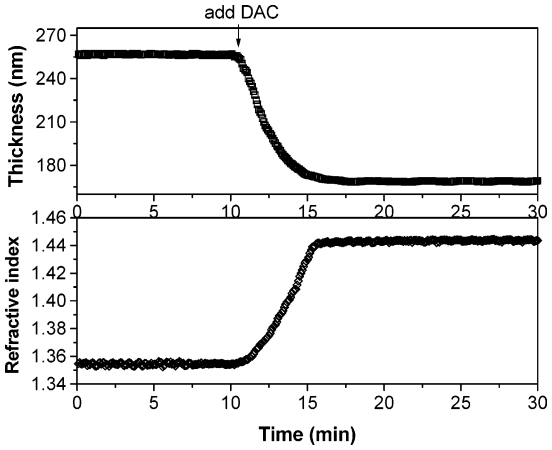

Figure 9. Ellipsometric measurements for the thickness and refractive index of a surface-grafted PLGA in the course of interaction with DAC in the 60 mL 2 mM pH 8 Tris buffer solution. A 0.5 mL 10 mM DAC solution was added to the liquid cell at 11 min (indicated as an arrow).

stretch), and 2854 cm^{-1} (strong, alkyl CH_2, symmetric, stretch) come from DAC.

To further confirm the coil-to-helix transition by binding with DAC, CD measurements were performed. Figure 8 shows the CD spectra of PLGA before and after binding with DAC in a pH 8 buffer. The spectrum in the absence of surfactant indicates a random-coil conformation. After binding with DAC, the CD spectrum has a double minimum at 208 and 222 nm, which is typical for the α-helical conformation.

Furthermore, Figure 9 shows the corresponding change of the film thickness and refractive index during the DAC binding process measured by ellipsometer in situ. Before the addition of DAC, the film has the thickness of 257 nm and a refractive index of 1.354. After the addition of DAC, the film thickness gradually decreases to 169 nm with the refractive index increasing to 1.443 simultaneously. The decrease of the film thickness is due to the conversion from an extended random-coil conformation to a compacted α-helical conformation. The increase of the refractive index is due to the shrinkage of PLGA main chains as well as the binding of long alkyl chains (10 carbons) with the carboxylic side groups. Both processes correspond to the coil-to-helix transition event measured by CD. The transition process takes about 5 min. This process is comparatively slower than that induced by pH, which is almost instantaneous. It is partially due to the relatively slow diffusion of DAC into the PLGA film and partially due to the slow rearrangement of the PLGA−DAC complex in the confined space.

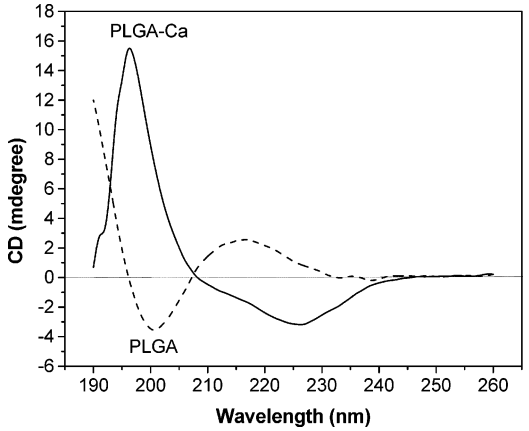

Figure 10. CD spectra of surface-grafted PLGA and PLGA−Ca complex in 2 mM pH 8 Tris buffer.

The conformational transition during the binding of DAC with the ionic PLGA films can be explained by the change of the electrostatic interaction in films.[43] The neutralization of the side chains leads to the formation of the α-helical structure.

The PLGA−DAC complex is stable at neutral pH. It can be dissociated quickly by adding competitive protons in solution. For example, the immersion of the film in a pH 4 buffer for 1 min can completely dissociate the PLGA−DAC complex.

3.5. Coil-to-Helix Transition Induced by Divalent Metal Ion (Ca^{2+}). The conformational transition of free PLGA can also be induced by divalent metal ions, such as Ca^{2+}, Mg^{2+}, Cd^{2+}, or Zn^{2+}.[31,32] In this study, we examine the effects of a biologically important ion, Ca^{2+}, on the surface-grafted films. Figure 10 shows the CD spectra of a surface-grafted PLGA before and after complexation with Ca^{2+} at pH 8. The PLGA−Ca complex adopts an α-helical conformation, as confirmed by the CD spectrum with a trough at 226 nm and a peak at 198 nm. This CD spectrum is distorted from the regular helical curve (shown in Figure 2a). This distortion might come from two sources: the CD contribution from the counterions and the helix percentage of PLGA−Ca.

Figure 11 shows the change of the film thickness and refractive index of a surface-grafted PLGA during binding with Ca^{2+}. Before the addition of Ca^{2+}, the PLGA film was random coiled at pH 8, with the film thickness of 262 nm and refractive index of 1.355. After the addition, the film thickness quickly decreased to 153 nm while the refractive index increased to 1.383. The decrease of film thickness was due to the change from extended random-coiled chains of the PLGA to the compact α-helical chains of the PLGA−Ca. The increase of refractive index was due to the shrinkage of PLGA chains. The transition process completed within 20 s. This process was much faster than that was induced by DAC (5 min). We attribute this to the faster diffusion of Ca^{2+} than DAC.

The effect of divalent ions on the PLGA conformation can be ascribed to the specific ion−macromolecule interaction between ion and carboxylate side groups, which decreases the electrostatic interaction. Thus, only a trace amount of divalent ions can induce this transition. As an approximate estimation, for each Ca^{2+} ion binding with two carboxylate groups on the PLGA with

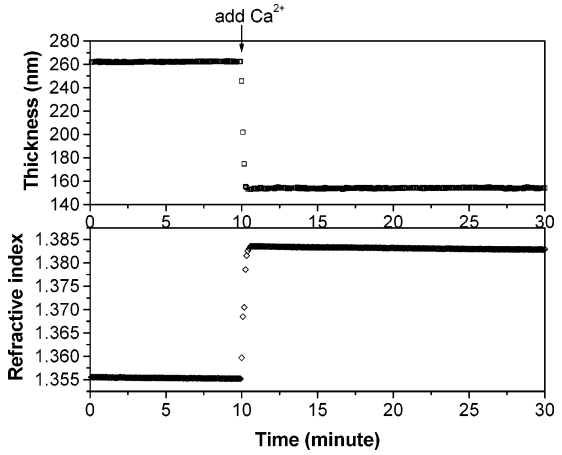

Figure 11. Thickness and refractive index of a surface-grafted PLGA in the course of complexation with Ca^{2+} measured by ellipsometry. A 60 mL 2 mM pH 8 Tris buffer was added to the liquid cell, followed by an addition of a 0.5 mL 10 mM $CaCl_2$ solution at 10 min (indicated as an arrow).

the DP of 1100, only ~90 nmol of Ca^{2+} can induce the coil-to-helix transition for a 1 cm^2 PLGA film.[44]

4. Conclusions

Surface-grafted PBLG films were synthesized by using SI-VDP of NCA of BLG. The conversion of PBLG to PLGA was completed by 1 h sonication in the HBr/benzene solution.

For the first time, we directly demonstrated the charge-induced conformational transitions for polypeptides in the surface-grafting state. pH (H^+/OH^-), surfactant (DAC), and divalent metal ion (Ca^{2+}) were chosen as the external stimuli. CD and ellipsometry were used to measure the conformational transitions of surface-grafted PLGA and the corresponding dielectric changes. These two instruments gave equivalent results, indicating the close association of conformations and surface properties.

The difference of transitional point pH_t between free state and surface-grafting state was ascribed to the additional free energy Δf_{extra} involved in the surface-grafting state. The experimental data were consistent with the existing theoretical models.

In general, the helix−coil transition of the surface-grafted films follows the similar patterns of that of the free state. However, because of the energy penalty, the helical state is preferable. These results do coincide with the theoretical prediction. On the other hand, because of the surface hindrance effect, the diffusivity of external stimulants becomes a more important limiting factor in controlling the kinetics of the conformational transition than those in the free state. In the future, a semiempirical model that combines both theory and experimental results should be established for better prediction. The implication of the current study offers insights into the community whose research involves biomolecular interfaces, such as binding assays and biosensors, and has the needs to correlate their observation from interfaces to the real world scenario. In addition, the surprising finding in the extreme responsiveness of the surface-grafted PLGA films could establish polypeptide materials as a new category of responsive biocompatible materials. These materials would be useful in creating new types of actuators, transducers, etc., for the future optic and electro applications.

Supporting Information Available: Experimental information on (1) chemicals, (2) cleaning of substrates, and (3) debenzylation. This material is available free of charge via the Internet at http://pubs.acs.org.

References and Notes

(1) Zimm, B. H.; Rice, S. A. J. *Mol. Phys.* **1960**, *3*, 391.
(2) Poland, D.; Scheraga, H. *Theory of Helix-Coil Transition in Biopolymers*; Academic Press: New York, 1970.
(3) Zhang, W.; Nilsson, S. *Macromolecules* **1993**, *26*, 2866.
(4) Grourke, M. J.; Gibbs, J. H. *Biopolymers* **1967**, *5*, 586.
(5) Sarkar, P. K.; Doty, P. *Proc. Natl. Acad. Sci. U.S.A.* **1966**, *55*, 981.
(6) Ponomarenko, E. A.; Tirrell, D. A.; MacKnight, W. J. *Macromolecules* **1996**, *29*, 8751.
(7) Puett, D.; Ciferri, A. *J. Phys. Chem.* **1967**, *71*, 4126.
(8) Alex, S.; Tajmir-Riahi, H. A.; Savoie, R. *Biopolymers* **1987**, *26*, 1421.
(9) Davidson, B.; Fasman, G. D. *Biochemistry* **1967**, *6*, 1616.
(10) Ali, S. *Polymer* **1978**, *19*, 229.
(11) Karasz, F. E.; O'Reilly, J. M.; Bair, H. E. *Nature (London)* **1964**, *202*, 693.
(12) Epand, R.; Scheraga, H. A. *Biopolymers* **1968**, *6*, 1383.
(13) Baier, R. E.; Zisman, W. A. *Macromolecules* **1970**, *3*, 70.
(14) Kugo, K.; Okuno, M.; Kitayama, K.; Kitaura, T.; Nishino, J.; Ikuta, N.; Nishio, E.; Iwatsuki, M. *Biopolymers* **1992**, *32*, 197.
(15) Pieroni, O.; Fissi, A.; Popova, G. V. *Prog. Polym. Sci.* **1998**, *23*, 81.
(16) Pieroni, O.; Fissi, A.; Angelini, N.; Lenci, F. *Acc. Chem. Res.* **2001**, *34*, 9.
(17) Jaworek, T.; Neher, D.; Wegner, G.; Wieringa, R. H.; Schouten, A. J. *Science* **1998**, *279*, 57.
(18) Chang, Y.-C.; Frank, C. W.; Forstmann, G. G.; Johannsmann, D. *J. Chem. Phys.* **1999**, *111*, 6136.
(19) Prucker, O.; Christian, S.; Bock, H.; Rüde, J.; Frank, C. W.; Knoll, W. *Macromol. Chem. Phys.* **1998**, *199*, 1435.
(20) Chang, Y.-C.; Frank, C. W. *Langmuir* **1998**, *14*, 326.
(21) Wang, Y.; Chang, Y.-C. *Langmuir* **2002**, *18*, 9859.
(22) Wang, Y.; Chang, Y.-C. *Adv. Mater.* **2003**, *15*. 290.
(23) Lee, N. H.; Frank, C. W. *Langmuir* **2003**, *19*, 1295.
(24) Nagasawa, M.; Holtzer, A. *J. Am. Chem. Soc.* **1964**, *86*, 538.
(25) McDiarmid, R.; Doty, P. *J. Phys. Chem.* **1966**, *70*, 2620.
(26) Olander, D. S.; Holtzer, A. *J. Am. Chem. Soc.* **1968**, *90*, 4549.
(27) Satake, I.; Gondo, T.; Kimizuka, H. *Bull. Chem. Soc. Jpn.* **1979**, *52*, 361.
(28) Maeda, H.; Kato, H.; Ikeda, S. *Biopolymers* **1984**, *23*, 1333.
(29) Hayakawa, K.; Nagahama, T.; Satake, I. *Bull. Chem. Soc. Jpn.* **1994**, *67*, 1232.
(30) Liu, J.; Takisawa, N.; Kodama, H.; Shirahama, K. *Langmuir* **1998**, *14*, 4489.
(31) Maeda, H.; Nakajima, J.; Oka, K.; Ikeda, S. *Int. J. Biol. Macromol.* **1982**, *4*, 352.
(32) Kurotu, T. *Inorg. Chim. Acta* **1991**, *191*, 141.
(33) Ben-Ishai, D.; Berger, A. *J. Org. Chem.* **1952**, *17*, 1564.
(34) Blout, E. R.; Idelson, M. *J. Am. Chem. Soc.* **1956**, *78*, 497.
(35) Buhot, A.; Halperin, A. *Europhys. Lett.* **2000**, *50*, 756.
(36) *Circular Dichroism and the Conformational Analysis of Biomolecules*; Fasman, G. D., Ed.; Plenum: New York, 1996.
(37) Elias, H.-G. *An Introduction to Polymer Science*, 1st ed.; VCH: New York, 1997.
(38) Nilsson, S.; Zhang, W. *Macromolecules* **1990**, *23*, 5234.
(39) Ito, Y.; Ochiai, Y.; Park, Y. S.; Imanishi, Y. *J. Am. Chem. Soc.* **1997**, *119*, 1619.
(40) Ito, Y.; Park, Y. S.; Imanishi, Y. *Langmuir* **2000**, *16*, 5376.
(41) Snipp, R. L.; Miller, W. G.; Nylund, R. E. *J. Am. Chem. Soc.* **1965**, *87*, 3547.
(42) Zimm, B. H.; Bragg, J. K. *J. Phys. Chem.* **1959**, *31*, 526.
(43) Satake, I.; Yang, J. T. *Biochem. Biophys. Res. Commun.* **1973**, *54*, 930.
(44) To estimate the mole of functional groups in the surface-grafted PLGA, suppose each PLGA chain occupies an area of 1 nm^2, and the chains are densely packed, and each chain has a DP of 1100. Thus, the mole of COO^- group is 177 $nmol/cm^2$.

MA034092Z